SIMULATION OF OIL SHALE RETORTING USING THE ICON© STEADY STATE MODEL

S.A. Zainal Abidin[a] *, O. Bekri[b], A. Jalaludin[a]
[a] PETRONAS Research & Scientific Services, Bangi, Malaysia
[b] Chapem Consultants, Rabat, Morocco
* Corresponding author (Email: azmanai@petronas.com.my)

The steady state process simulation software iCON©, developed by PETRONAS, is based on a thermodynamic and physical property calculation mechanism and is mainly used to predict process behavior for upstream and downstream oil and gas applications.

Since iCON© has various heavy oil property packages specific to the industrial process requirements, the aim of this work is to apply this simulation tool to the oil shale retorting process. The iCON© model is constructed based on the results of retorting of the Moroccan Timahdit oil shale samples using thermo-gravimetric analyzers (TGA). This model predicts the product of the oil shale retorting process from a specific shale feed. The product of this pyrolysis process will include vapor products (oil, gas and liquid water before condensation) and spent shale (which includes carbon residue).

Future studies will include applying this model to other oil shale samples which would differ in its characteristics and set of reaction kinetics.

1. INTRODUCTION

Oil Shale deposits around the globe have been utilized in various commercial forms since early 20th century. However, their use as an alternative source of fuel to conventional oil has been limited. Among the limitations that are withholding the commercialization of shale oil include the fluctuating oil prices and the development of reliable and efficient oil shale technology. The current trend of crude oil price increase in the global market has renewed an interest in this energy source despite its relatively low processing efficiencies and adverse environmental impacts based on current technology. Oil shale deposits are known to have varying composition and oil yields. The ability to manage the waste from shale processing and to optimize the upgrading process of shale oil produced from the shale deposits would contribute to extensive exploitation of the abundant reserves available. Process simulation provides a tool to optimize the production of shale oil.

PETRONAS, with its policy on diversifying liquid hydrocarbon sources, is pursuing to develop competencies in oil shale technology. The company is determined to undertake various opportunities in the oil and gas sector especially in exploring various alternative energy sources.

This paper focuses on developing a model for the retorting (or pyrolysis) process of oil shale. A graphical user interface (GUI) was developed in Microsoft Visual Basic® as it is readily attached with iCON©, the steady state simulation software of PETRONAS. Data required for this paper were obtained from previous lab-scale study which utilized Moroccan Timahdit oil shale samples using a thermo-gravimetric analyzer (TGA). The results using TGA were later compared to results of Fischer Assay tests and fluidized bed retort process tests.

This model predicts the formation of oil and gas on the basis of heating of the shale regardless of the retorting technique used.

2. METHODOLOGY

The model was developed based on the decomposition reactions of kerogen and bitumen. Kerogen is an insoluble organic component of shale. The temperature at which kerogen is released as indicated in Table 1 has been used in the model.

Table 1: Decomposition temperature range

Component	Temperature Range (ºC)
Kerogen	270-320
Bitumen	350-550
Dolomite	650-750
Calcite	720-850

Equation 1 represents the basic reaction of the organic matter decomposition. Continuous heating of the oil shale will further decompose the kerogen into bitumen as well as oil and gas.

$$Kerogen \xrightarrow{k_1} \begin{matrix} oil\ \&\ gas \\ bitumen \end{matrix} \xrightarrow{k_2} \begin{matrix} oil\ \&\ gas \\ residual\ \ carbon \end{matrix} \qquad (1)$$

Further heating will result in decomposition of the carbonates (calcites and dolomites) to form carbon dioxide as well as Calcium and Magnesium Oxides respectively. Residual carbon is produced during the decomposition of kerogen and bitumen but has been neglected for kerogen decomposition to simplify the model. The amount of kerogen and bitumen that could be produced is highly dependant on the organic content of the shale. A table representing the organic matter characterization of Layer M1 Timahdit shale sample is as follows:

Table 2: Characteristics of Timahdit sample (Layer M1) in wt% (Bekri, O., 1996)

Sample	**Mo**
General Characteristics	
Organic Matter (%)	15.28
Ash (%)	61.85
Density @ 20ºC (kg/m^3)	2.28
Total Carbon (%)	15.9
Mineral Carbon (%)	6.07
Organic Carbon (%)	9.83

The methodology for developing the model is based on the experimental TGA results as well as a set of mathematical equations as expressed below.

2.1. Experimental Methodology

A major expected function of the model is to accept data from experimental laboratory results which would be used to estimate the total amount of oil and gas produced. The model would be made to accept data from processes using any type of heating. The laboratory analysis data for this model are based on results from the TGA. TGA is conducted by using equipment that measures the weight loss of a sample as a function of time and under temperature control. TGA analysis can be performed isothermally or non-isothermally. The information available for this paper employed the non-isothermal TGA analyses.

The TGA would require sample mass of less than 20mg, pre-crushed to fine particles of less than 150μm in diameter. A chart representing sample weight loss with temperature, at each heating rate, is plotted for each tested shale sample. The data obtained from these TGA charts would be used to run the model. The rate of weight loss over temperature and the peaks obtained for each heating rate would be the raw data in calculating kerogen and bitumen decomposition rates. Figure 1 represents the chart of sample weight versus temperature for each heating rate for M Zone of Timahdit shale.

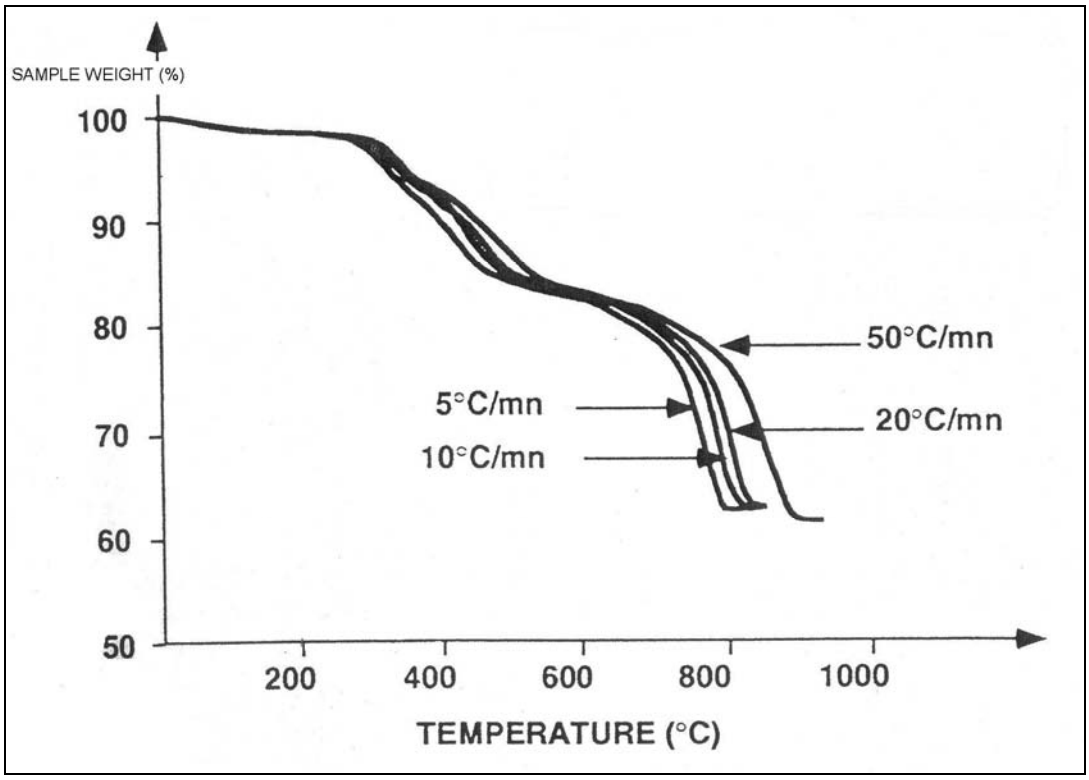

Figure 1: An example of TGA Chart (Bekri, O., 1996)

Figure 2 represents the rate of weight loss of sample over temperature for the same shale sample. The chart provides the values dP/dT for the mathematical calculations. This chart is different from that in Figure 1.

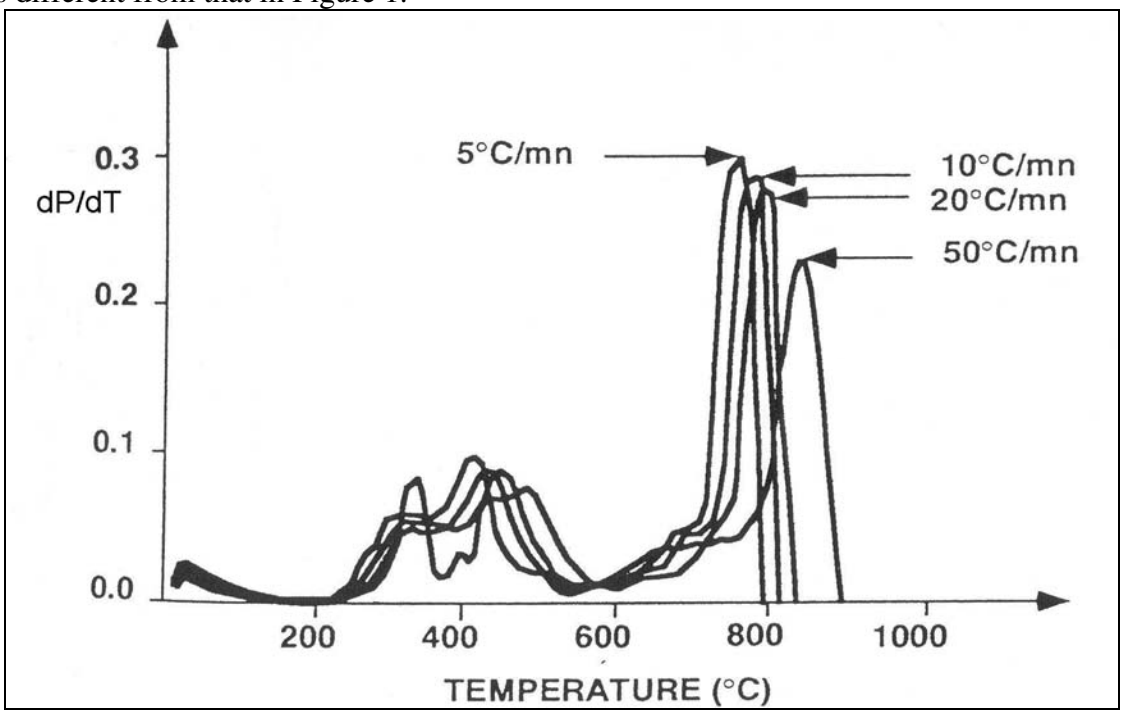

Figure 2: An example of dP/dT Chart for Timahdit Shale Zone Mo (Bekri, O., 1996)

2.2. Mathematical Modeling

There are various assumptions made in the mathematical calculations for the model. These assumptions are necessary to simplify the calculations involved as a base for the modeling process. An assumption made was that there is no change in particle size throughout the pyrolysis process. For the non-isothermal tests, it was assumed that there is always a temperature differential ($\delta T/\delta t \neq 0$). It was also assumed that there is constant heat and mass transfer in the sample.

Kerogen Decomposition

The calculation for kerogen decomposition is outlined below with the following terminologies:
dP/dT: weight loss over temperature for sample
V: heating rates (ºC/min)
Mo: initial fraction of organic material in the shale
P: mass fraction of sample at temperature T
T: selected temperatures for kerogen decomposition *(K)*
R: Universal Gas Constant taken as *8.314 J/gmol.K*
E_1: activation energy for the rate of decomposition of kerogen
k_{10}: frequency factors in Arrhenius equation where $k_1=k_{10}e^{-E1/RT}$
f_1: fraction of kerogen decomposition into oil & gas

Step 1
First, we have to consider f_1 which depends on the heating rate. Bitumen decomposition is neglected in the decomposition calculations for kerogen.
Equation (2) as denoted by the following equation was derived from several correlations of the kerogen decomposition reactions:

$$\ln\left(-V\frac{dP}{dT}\right)=-\frac{E_1}{RT}+\ln\left(Mo.f_1.k_{10}\right)-\left(\frac{k_{10}.RT^2}{E_1}.e^{-E_1/RT}\right).\frac{1}{V} \qquad (2)$$

Therefore, to form a correlation, plot $\ln\left(-V\frac{dP}{dT}\right)_{T=cons\tan t}$ as a function of *1/V*. The slope represents *A1 (T)* and the y-intercept *B1 (T)* which is determined from the least square method.

$$A1(T)=-\frac{k_{10}}{E_1}RT^2.e^{-E_1/RT} \qquad (3)$$

$$B1(T)=-\frac{E_1}{RT}+\ln(Mo.f_1.k_{10}) \qquad (4)$$

Step 2
Equation 3 and 4 would require certain information to be able to solve for k_{10} and E_1 which would eventually provide results for f_1. Hence, equation (4) is utilized by plotting *B1 (T)* as a function of *1/T* which will provide the slope *A2* and intercept *B2*:

$$A2 = -E_1/R \text{ so } E_1 = -A2.R \qquad (5)$$

$B2 = ln\ (Mo.f_1k_{10})$ (6)

Equation (5) provides the value of E_1 which can be utilized in equation (3) to calculate $k_{10.}$

By rearranging equation (3), equation (7) is obtained:

$k_{10}= (E_1.A1\ (T)/RT^2)\ e^{E_1/RT}$ (7)

Step 3

Steps 1 and 2 allow us to calculate E_1 and k_{10}

Equation (8) is then rearranged to calculate the factor f_1 for various heating rates as selected during the experimental stage.

$$P = 1 - V\frac{dP}{dT}\frac{e^{E1/RT}}{k_{10}} - Mof_1 \quad (8)$$

Step 4

Rearranging equation (2) and plotting the left hand side of the equation as a function of *1/V*, will be an iteration calculation for the values of k_{10} and f_1 to refine these values.

Values of E_1, k_{10} and f_1 from Steps 1-3 are used in calculating Equation (9).

$$\ln\left(-V\frac{dP}{dT}\right) - \ln\left(Mo.f_1.k_{10}\right) = -\frac{E_1}{RT} - \left(\frac{k_{10}.RT^2}{E_1}.e^{-E_1/RT}\right).\frac{1}{V} \quad (9)$$

From the result of equation (9), we obtain the slope *A3 (T)* and the intercept *B3 (T).*

$$A3(T) = -\frac{k_{10}}{E_1}RT^2.e^{-E_1/RT} \quad (10)$$

$$B3(T) = -\frac{E_1}{RT} \quad (11)$$

Equation (11) is used to calculate a new value of E_1, with this new value of E_1, equation (10) is used to calculate a new k_{10} value.

Step 5

From equation (8) and the new values of E_1 and k_{10} obtained from step 4, the new values for the factors f_1 are calculated at various heating rates

Step 6

Step 4 is repeated and the cycle is repeated until you obtain a constant value for E_1, k_{10} and f_1. The converged values will then be used as final values for further calculations.

Bitumen Decomposition

In the study of bitumen decomposition, it is assumed in the process that kerogen concentration is negligible. The terms in bitumen decomposition other than those described in kerogen decomposition include:
k_2: reaction rate constants following Arrhenius equation
P_o: mass fraction of sample at temperature where organic matter decomposition terminates
f_2: fraction of bitumen decomposition into oil & gas

The decomposition of bitumen is derived from the following rate of weight loss equation:

$$\frac{dP}{dT} = \frac{1}{V} k_{20} . e^{-E_2/RT} . (P - Po) \qquad (12)$$

Reducing equation (12), one has:

$$\ln\left(-\frac{V}{P - Po} . \frac{dP}{dT} \right) = -\frac{E_2}{RT} + \ln(k_{20}) \qquad (13)$$

Plotting the left hand side of equation (13) as a function of *1/T* gives a slope of
$A4 = -E_2/R$
$B4 = ln\ (k_{20})$

A4 and *B4* allow us to calculate the values of k_{20} and E_2.

An equation to represent production of oil and gas from the organic material, as a balance from the kerogen decomposition is derived from the following equation:

$$1 - Po = Mof_1 + Mo(1 - f_1) f_2 \qquad or \qquad f_2 = \frac{1 - Po - Mo.f_1}{Mo.(1 - f_1)} \qquad (14)$$

This expression permits us to calculate the fraction of bitumen converted to oil & gas (f_2) and fraction of kerogen converted to oil & gas (f_1) for different heating rates.

3. ICON© MODEL

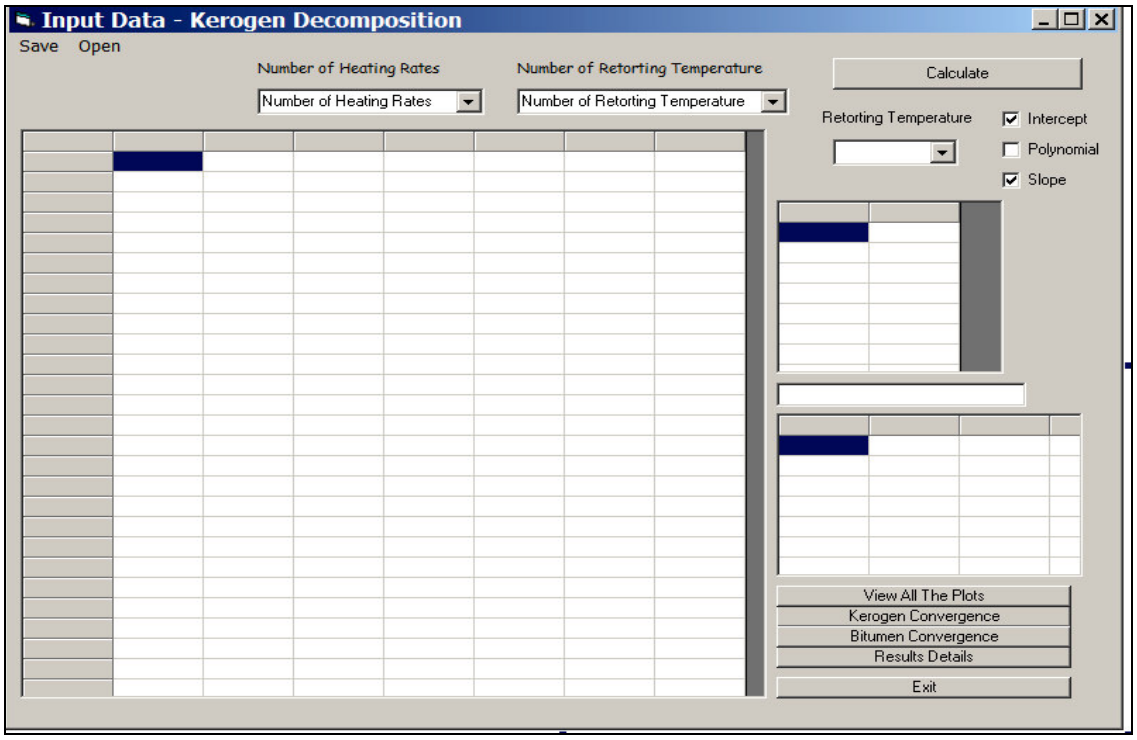

Figure 3: Shale Oil model startup form

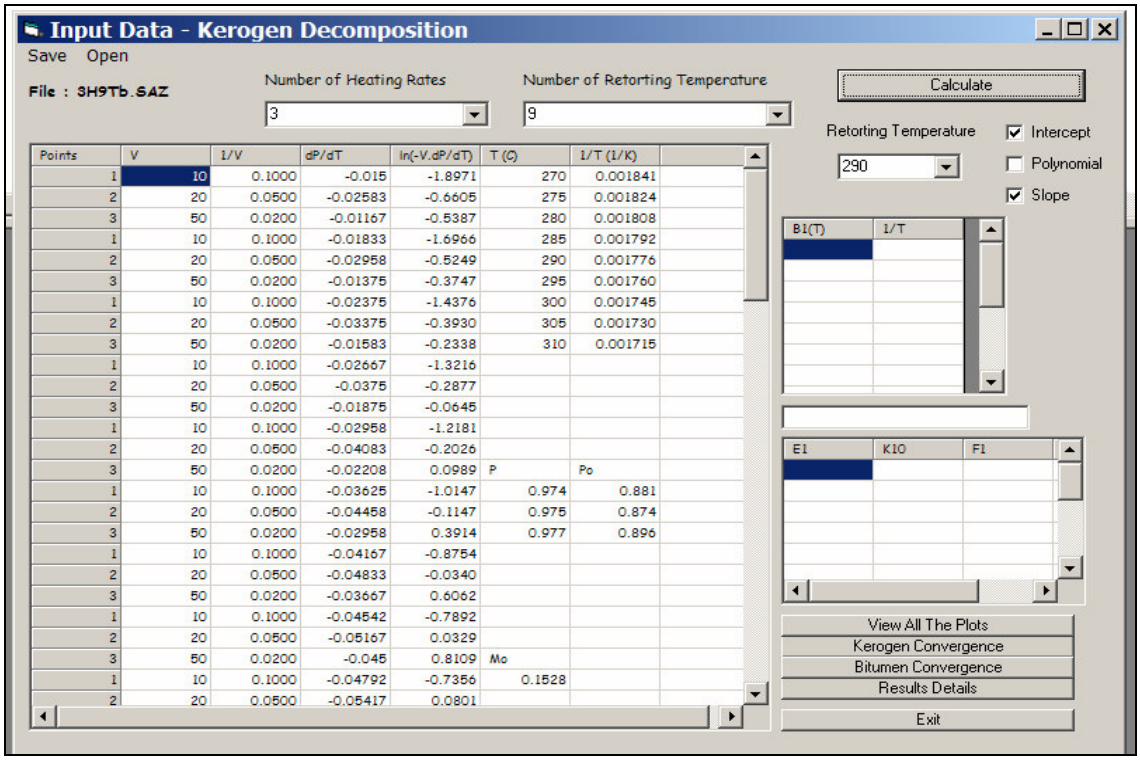

Points	V	1/V	dP/dT	ln(-V.dP/dT)	T (C)	1/T (1/K)
1	10	0.1000	-0.015	-1.8971	270	0.001841
2	20	0.0500	-0.02583	-0.6605	275	0.001824
3	50	0.0200	-0.01167	-0.5387	280	0.001808
1	10	0.1000	-0.01833	-1.6966	285	0.001792
2	20	0.0500	-0.02958	-0.5249	290	0.001776
3	50	0.0200	-0.01375	-0.3747	295	0.001760
1	10	0.1000	-0.02375	-1.4376	300	0.001745
2	20	0.0500	-0.03375	-0.3930	305	0.001730
3	50	0.0200	-0.01583	-0.2338	310	0.001715
1	10	0.1000	-0.02667	-1.3216		
2	20	0.0500	-0.0375	-0.2877		
3	50	0.0200	-0.01875	-0.0645		
1	10	0.1000	-0.02958	-1.2181		
2	20	0.0500	-0.04083	-0.2026		
3	50	0.0200	-0.02208	0.0989	P	Po
1	10	0.1000	-0.03625	-1.0147	0.974	0.881
2	20	0.0500	-0.04458	-0.1147	0.975	0.874
3	50	0.0200	-0.02958	0.3914	0.977	0.896
1	10	0.1000	-0.04167	-0.8754		
2	20	0.0500	-0.04833	-0.0340		
3	50	0.0200	-0.03667	0.6062		
1	10	0.1000	-0.04542	-0.7892		
2	20	0.0500	-0.05167	0.0329		
3	50	0.0200	-0.045	0.8109	Mo	
1	10	0.1000	-0.04792	-0.7356	0.1528	
2	20	0.0500	-0.05417	0.0801		

Figure 4: Pre-entered data for 9 temperatures and 3 heating rates

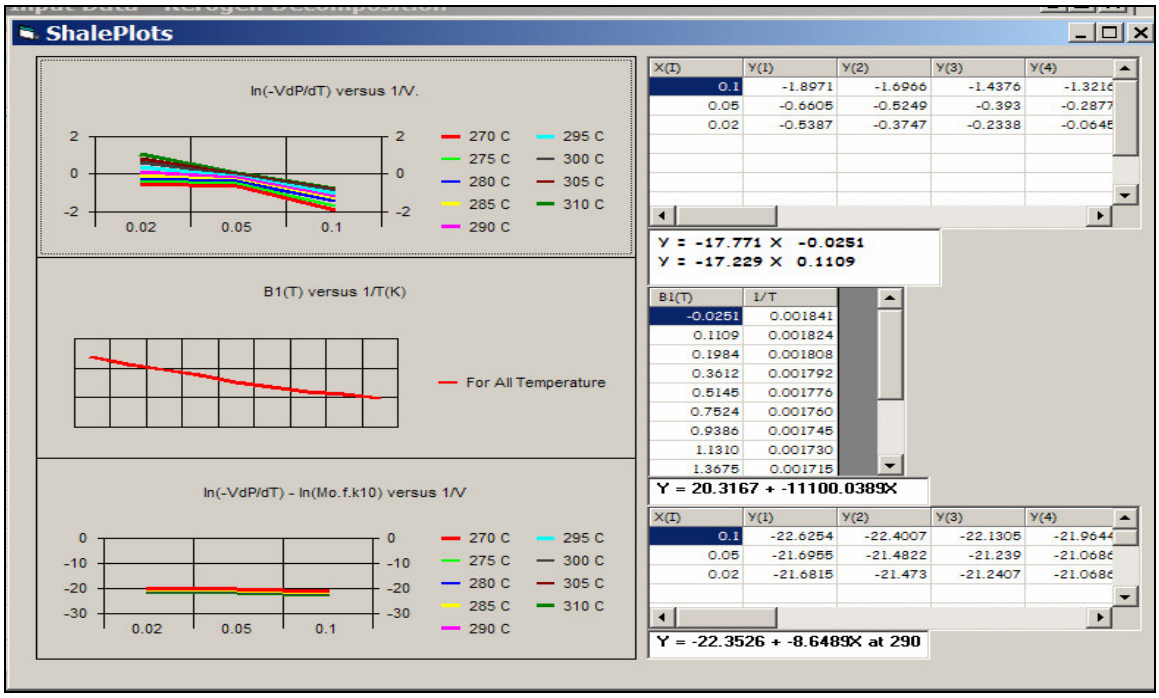

Figure 5: Form reviewing the plots

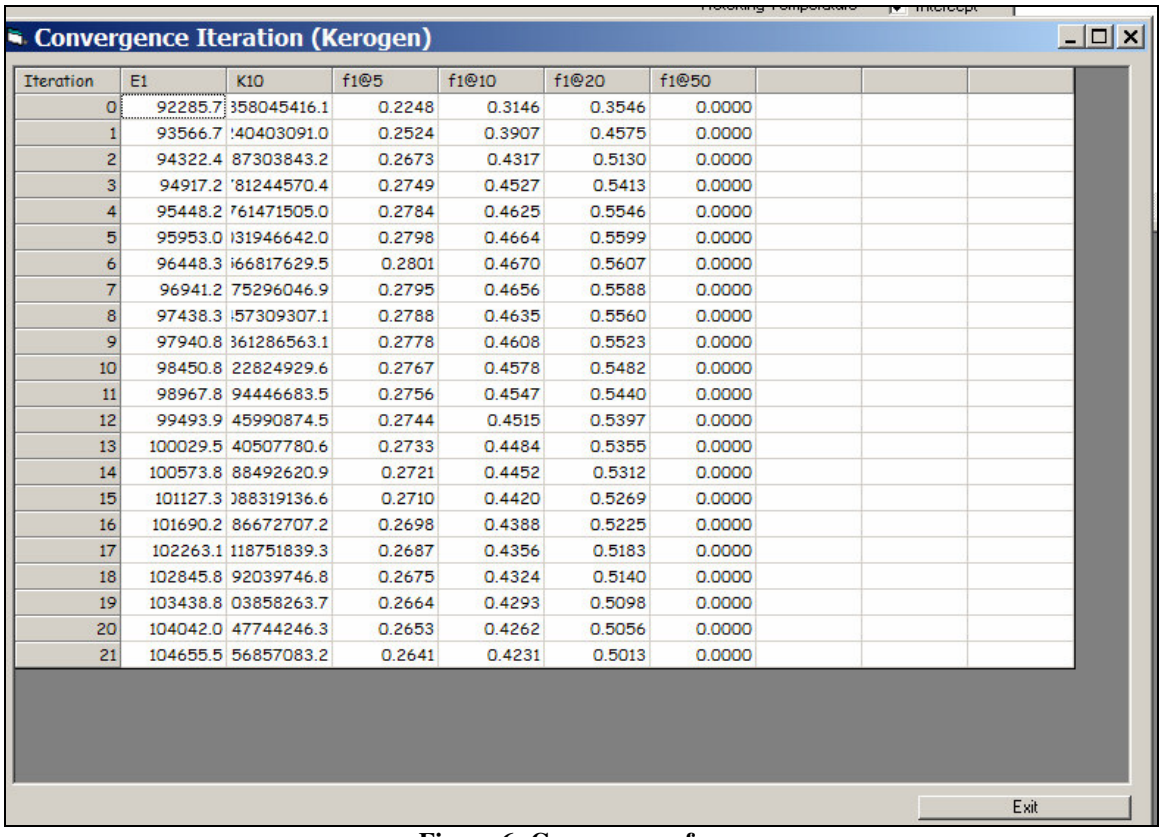

Iteration	E1	K10	f1@5	f1@10	f1@20	f1@50
0	92285.7	358045416.1	0.2248	0.3146	0.3546	0.0000
1	93566.7	140403091.0	0.2524	0.3907	0.4575	0.0000
2	94322.4	87303843.2	0.2673	0.4317	0.5130	0.0000
3	94917.2	81244570.4	0.2749	0.4527	0.5413	0.0000
4	95448.2	761471505.0	0.2784	0.4625	0.5546	0.0000
5	95953.0	131946642.0	0.2798	0.4664	0.5599	0.0000
6	96448.3	166817629.5	0.2801	0.4670	0.5607	0.0000
7	96941.2	75296046.9	0.2795	0.4656	0.5588	0.0000
8	97438.3	157309307.1	0.2788	0.4635	0.5560	0.0000
9	97940.8	361286563.1	0.2778	0.4608	0.5523	0.0000
10	98450.8	22824929.6	0.2767	0.4578	0.5482	0.0000
11	98967.8	94446683.5	0.2756	0.4547	0.5440	0.0000
12	99493.9	45990874.5	0.2744	0.4515	0.5397	0.0000
13	100029.5	40507780.6	0.2733	0.4484	0.5355	0.0000
14	100573.8	88492620.9	0.2721	0.4452	0.5312	0.0000
15	101127.3	088319136.6	0.2710	0.4420	0.5269	0.0000
16	101690.2	86672707.2	0.2698	0.4388	0.5225	0.0000
17	102263.1	118751839.3	0.2687	0.4356	0.5183	0.0000
18	102845.8	92039746.8	0.2675	0.4324	0.5140	0.0000
19	103438.8	03858263.7	0.2664	0.4293	0.5098	0.0000
20	104042.0	47744246.3	0.2653	0.4262	0.5056	0.0000
21	104655.5	56857083.2	0.2641	0.4231	0.5013	0.0000

Figure 6: Convergence form

4. RESULTS AND DISCUSSION

The experimental data utilized in this paper were based on non-isothermal TGA tests. However, in the case that an isothermal TGA test is conducted, the sample is heated to the required temperature and the product is analyzed. However, the pre-heating stage is non-isothermal and would produce inaccurate results when compared to non-isothermal methods. In non-isothermal methods, the sample is heated at constant heating rates while monitoring the weight loss. The non-isothermal method is employed, as it requires less time even though a disadvantage is the difficulty to conclude an analysis where the production distribution and reaction constants may be dependant on the heating rate. A limitation in TGA analysis is the inability to characterize the oil and gas into detailed chemical composition (Bekri, O. et al, 1983). Nevertheless, TGA is a useful tool in analyzing the kinetics of the decomposition reactions and the non-isothermal method allows quick results as compared to other available methods.

Table 3 shows the kinetic parameters of the TGA analysis which are represented by the k_1 and k_2 values calculated based on the methodology provided.

The reaction rate constants for Timahdit M Zone shale are

$$k_1 = 2.8\times10^4 e^{-9.35/T} \quad (15)$$

$$k_2 = 4.8\times10^5 e^{-13.98/T} \quad (16)$$

Table 3: Kinetic parameters for the decomposition of organic material (Bekri, O., 1996)

	E_1(kJ/mole)	k_{10} (sec^{-1})	E_2(kJ/mole)	k_{20}(sec^{-1})
Zone M1	77.7	2.8 x10^4	116.2	4.8 x10^5

Tables 4 and 5 represent the constant rates at different temperatures for the decomposition of kerogen and bitumen respectively. These tables indicate the temperature dependence of the decomposition reactions of kerogen and bitumen. It was also proven in the model that the rate constants are highly dependant on temperature as various temperatures selected as the basis for the iteration process provided varying results.

Table 4: Constant rates for the decomposition of kerogen at different temperatures (k_1 x 1000(1/s)) (Bekri, O., 1996)

T(ºC)	275	300	350	400	450	500
Zone M1	1.08	2.3	8.55	26.07	68.13	157.3

Table 5: Constant rates for the decomposition of bitumen at different temperatures (k_2 x 1000(1/s)) (Bekri, O., 1996)

T(ºC)	350	400	450	500	550
Zone M1	0.08	0.45	1.9	6.62	19.9

Table 6 represents the fraction of kerogen and bitumen that is converted to oil and gas. It is noticeable that the conversion rates increase with heating rate. This is expected as more oil and gas can be released upon addition of an increased amount of heat energy. The

results also show that the f_2 values are higher than f_1 values. This is because f_1 represents the conversion rate of kerogen into bitumen as well as oil and gas. Therefore a large portion of the kerogen would also form bitumen and carbon residues other than oil and gas compared to f_2 where the bitumen only decomposes to oil and gas and residual carbon. An operating range of 350-550 ºC also contributes to the high conversion rates of bitumen into oil and gas.

Table 6: Fraction of kerogen (f_1) and bitumen (f_2) converted to oil, gas and carbon residue (Bekri, O., 1996)

Heating Rate (ºC/min)	5	10	20	50
M1: f_1	0.21	0.24	0.32	0.52
M1: f_2	0.84	0.86	0.88	0.93

Table 7 represents the total oil and gas produced from kerogen and bitumen. The table proves that a higher heating rate will result in higher oil and gas yields. This is due to the presence of an increased amount of heat energy as heating rate increases.

Table 7: Fraction of kerogen and bitumen converted to oil, gas and residual carbon (%wt) (Bekri, O., 1996)

Heating Rate (ºC/min)	5	10	20	50
Zone M1				
Oil & Gas originating from kerogen = $100f_1$	21.00	24.00	32.00	52.00
Oil & Gas originating from bitumen = $(1-f_1).100f_2$	66.36	65.36	59.84	44.64
Total Oil & Gas	87.36	89.36	91.84	96.64
Carbon Residue	12.64	11.64	8.16	3.36

The methodology for the decomposition of kerogen is a highly simplified method. It has neglected the presence of hydro-cracking and hydro-coking reactions. This is based on the limitations of the TGA results which could not allow a chemical composition analysis of the final or intermediate products to be performed due to the small sample size used in the experiments. This is also a reason why the results of TGA analysis could not be directly related to chemical composition analyses of oil and gas products from other available experiments of shale pyrolysis as there is a difference in experimental methodologies. Among the methodological differences include varying range of particle sizes of initial sample mass, heat and mass transfer rates in the process and reactor design. A more detailed equipment design or a more complex mathematical model to include compositional analysis is necessary to relate the oil and gas product of this model to a more extensive chemical composition analysis. This will be required in future developments to assist in process improvements and control mechanisms especially in plant environments. Examples of methods to obtain detailed characterization of the products include gas chromatography and infra-red (IR) spectroscopy.

Table 8 shows a comparison between TGA results, Fischer Assay results and fluidized bed results (Sadiki et al, 2003). The table also compares the effects of particle size on the production of oil and gas from oil shale samples.

Table 8: Comparison of results from different tests

Sample	Layer M1		Layer Y	
TEST	**Fischer Assay**	**TGA (5ºC/min~50ºC/min)**	**Fluidized Bed**	**Fischer Assay**
Sample Size	100 g	20mg	1.3 kg/hr	100g
Particle Size	3.3mm	<150 µm	300-400 µm	3.3mm
Oil	7.2	13.3 ~ 14.8	16.5	11.3
Gas	2.4		6.0	3.7
Water	1.8		2.8	2.8
Carbon Residue	3.9	1.9 ~ 0.5	2.7	6.2
Spent Shale (Mineral)	84.7	84.8 ~ 84.7	72.1	76.0
Spent Shale (Total)	88.6	86.7 ~ 85.2	74.7	82.2

-Layer M1 Timahdit shale has an organic matter content of 15.28% (Bekri, O, 1996)
-Fluidized bed on Timahdit sample utilizing 3kg/hr Hamburg continuous bench-scale facility (Sadiki et al, 2003)
-Layer Y Timahdit shale has an organic matter content of 24% (Bekri, O., 1996)

The results from the above table show that particle size and reactor design (based on sample size) has an effect on oil and gas formation. The fluidized bed method produces a larger amount of oil and gas compared to the TGA and Fischer Assay results. However, this is because Layer Y of Timahdit sample has 57% more organic matter than Layer M1 samples.

The difference in particle size and reactor design also has an influence on product formation. The fluidized bed would have a higher product formation rate due to the fluidization process involved as well as having a rather small particle size compared to the Fischer Assay tests. The fluidized bed managed to produce an oil ratio compared to Fischer Assay of 146. The TGA test is also able to produce more oil and gas than Fischer Assay as the sample has been crushed to fine particles of less than 150 µm in diameter. This allows better heat transfer, which provides the necessary energy for organic matter decomposition. Comparing the TGA and fluidized bed results, it is obvious that the fluidized bed results are higher than TGA even though TGA has smaller particle size, which should allow higher decomposition rates. However, the results are inconclusive as the factors of particle size, sample organic matter content as well as heat and mass transfer have to be taken into consideration. Nevertheless, the expectation that other methods could produce more oil and gas than Fischer Assay tests is proven.

The model being tested for samples T, M and X+Y zones of Moroccan Timahdit shale proves the flexibility of the model in utilizing various shale samples. However, the model also indicates that the results (f_1 and f_2 values) are sensitive to entered data. Hence, errors in extracting information from the TGA charts should be kept to a minimum. The model also allows the user to select a temperature to evaluate f_1. This feature would be useful in allowing the user to determine the most suitable temperature for optimum f_1 and f_2 results.

5. CONCLUSION

The model for oil shale processing was based on the simplified kerogen and bitumen decomposition reactions. The parameters to be calculated from this model are the conversion of kerogen and bitumen into oil and gas, which were represented by the values of f_1 and f_2. The production of residual carbon from the decomposition of kerogen had also been ignored to simplify calculations. The hydro-cracking and hydro-coking products from shale oil pyrolysis were discarded in the model.

The raw data obtained from the TGA analysis of Tarfaya and Timahdit shale oil samples were used to validate the model that had been developed using Microsoft Visual Basic ®. It was proven that the model is true for any type of heating. The major limitation of the non-isothermal TGA analysis as the basis for this model was the inability to characterize the oil and gas composition due to the small sample mass used in the TGA.

Product oil and gas characterization as well as the inclusion of the reaction mechanisms of hydro-cracking and hydro-coking should be a feature to be considered. This could only be possible by incorporating a more complex and detailed mathematical model for the decomposition reactions and possibly using other experimental methods, which are able to characterize the products.

Further development is necessary to produce a more accurate and robust model which can be used as a tool to predict oil and gas production capacity for a given shale sample.

6. LIMITATIONS OF STUDY & FUTURE WORKS

The shale oil industry is strongly dependant on the global oil price due to the lower price of the oil and gas produced from shale processing. Therefore a stable oil price is necessary to ensure the economic feasibility of the industry as well as interest in shale oil research and development.

The paper has indicated the oil shale technology as a major limitation in its exploitation. Therefore, further research in the areas of environmental waste management and process design to improve efficiency is a profound necessity to ensure that the oil shale industry is an economically and environmentally feasible option.

At the present stage, only the study of the kerogen and bitumen decomposition reactions in developing the model is considered and this model is subject to various limitations. Data from the charts are subject to errors and these errors should be minimized to obtain more accurate results. Future studies should also include the effects of mineral decomposition on oil and gas production rates.

The model should also be validated with existing shale mathematical models.
The model being based on a non-isothermal operation should also be compared to isothermal operations or use of fluidized bed methods. Another major limitation is the

inability of the model to characterize the production of oil and gas and the elimination of hydro-cracking and hydro-coking reactions. It would be a significant progress to include a more detailed reaction set as part of the model. This might include developing a new experimental methodology and a more detailed mathematical derivation. A physical and chemical characterization with kinetics and reaction mechanisms would also assist in the development of a more comprehensive model.

The effect of particle size, mass and heat transfer and reactor design on shale decomposition was studied on a basic scale as a means of comparison and validation of the model. A comprehensive work comparing different experimental methodologies to be used for this model would be included in future studies. This however would require complex mathematical derivations and time.

The decomposition of inorganic carbonates into carbon dioxide and inorganic oxides has also been neglected and should be included in future works as the fraction of this product is rather significant.

The model would be further improved to increase robustness and user friendliness. The model would be embedded into iCON© where further trials would be conducted and downstream processing of the shale oil would be possible.

References

1. Bekri O., Baba Habib M.H., et Col., *Study of Moroccan Oil Shale Thermal Decomposition Kinetics,* Proceedings of the 16th Colorado School of Mines Oil Shale Symposium, Golden, Colorado, April 1983.
2. Bekri O., 1996, *Characteristics and physical chemistry of Timahdit and Tarfaya Shale*, Mohamed V University, Rabat , Morocco.
3. Sadiki A. et al, 2003,*Fluidised Bed Pyrolysis of Moroccan Oil Shales using the Hamburg Pyrolysis Process*, Journal of Analytical and Applied Pyrolysis, Vol 70, Issue 2, pp 427-435.